Chapter 12

Benchmarks for Non-Ideal Magnetohydrodynamics

Sofronov Vasily, Zhmailo Vadim and Yanilkin Yury

Additional information is available at the end of the chapter

http://dx.doi.org/10.5772/intechopen.75713

Abstract

The paper presents an overview of benchmarks for non-ideal magnetohydrodynamics. These benchmarks include dissipative processes in the form of heat conduction, magnetic diffusion, and the Hall effect.

Keywords: ALE method, numerical simulation, magnetohydrodynamics, benchmark, verification

1. Introduction

Numerical modeling of magnetohydrodynamics (MHD) is an important and challenging problem addressed in numerous publications (e.g., see [1, 2]). This problem is further complicated in case of multi-flux models that account for the relative motion and interaction of particles of different nature (electrons, various species of ions, neutral atoms, and molecules) both with each other and with an external magnetic field.

This class of problems is generally solved using the fractional-step method, when complex operators are represented as a product of operators having a simpler structure. Thus, within the splitting method, the calculation of one-time step consists of a series of simpler procedures. It is obvious that difference schemes for each splitting stage should, where possible, preserve the properties of corresponding difference equations.

Note that the task of constructing reference solutions accounting for the whole range of physical processes is challenging (and often unfeasible). Existing benchmarks enable accuracy assessment of individual splitting stages rather than the simulation as a whole.

Magnetohydrodynamic problems are naturally divided into two groups: problems for an ideal infinitely conducting plasma and problems with dissipative processes in the form of heat conduction and magnetic viscosity.

Numerous publications on the construction of difference methods for ideal magnetohydrodynamics use a standard set of test problems. These include propagation of one-dimensional Alfven waves at various angles to grid lines [3–5], Riemann problem for MHD equations [6–9], and various two-dimensional problems accounting for the presence of a uniform magnetic field [3, 5, 10]. In [11], a number of additional ideal MHD benchmarks are presented, which are basically shock-wave problems. A special class of tests includes problems with a weak magnetic field not affecting the medium motion. If there is an exact solution for a given hydrodynamic problem, the magnetic field "freezing-in" principle allows finding components of the field $\mathbf{H}\left(H_x, H_y, H_z\right)$ at any time with the known medium displacements $\mathrm{X} = \mathrm{X}(\mathrm{X}_0, t)$.

The representation in publications of the problem of testing the dissipative stage of MHD equations is much the worse. Possibly, this is owing to complexity problems that require accounting the interaction of the shock-wave processes, heat conduction, diffusion of magnetic field, and Joule heating.

Numerical simulations of some of the tests presented here have been done using the Lagrangian-Eulerian code EGIDA developed at VNIIEF [12, 13] for multi-material compressible flow simulations.

The magnetohydrodynamic equation system in one-temperature approximation modified by the Hall effect can be written in the following conservative form [2]:

$$\begin{gathered}
\frac{\partial \rho}{\partial t} + div\rho\mathbf{u} = 0, \quad \frac{\partial \rho\mathbf{u}}{dt} + \mathrm{div}(\rho\mathbf{u}\otimes\mathbf{u} + (P+P_H)I - 0.5\mathbf{H}\otimes\mathbf{H}) = 0, \quad P_H = 0.5|\mathbf{H}|^2, \\
\frac{\partial H}{\partial t} + \mathrm{div}(\mathbf{u}\otimes\mathbf{H} - \mathbf{H}\otimes\mathbf{u}) = -rot(\nu\cdot rot\mathbf{H} + b[\mathbf{H}\times rot\mathbf{H}]), \quad \frac{\partial \rho n_\varepsilon}{\partial t} + \mathrm{div}(\rho n_\varepsilon \mathbf{u}) = 0, \\
\frac{\partial \Xi}{\partial t} + \mathrm{div}((\Xi + P + P_H)\mathbf{u} - \mathbf{H}(\mathbf{u}\cdot\mathbf{H}) - \kappa grad T) = 0, \quad \Xi = \rho\left(e + 0.5|\mathbf{u}|^2\right) + P_H, \\
P = P(\rho, T), \quad \varepsilon = \varepsilon(\rho, T).
\end{gathered} \tag{1}$$

where $\nu = c^2/(4\pi\sigma)$ is the magnetic viscosity coefficient, κ is the heat conduction factor, $b = c/(4\pi e n_e)$ is a local exchange (Hall) parameter [2], and e and n_e are charge and density of electrons. When writing Eq. (18), we assume that bias currents and electron inertia are negligibly small [2]. Equation system (1) differs from equation system for ideal MHD owing to diffusion terms present in the equations of energy and inductance of magnetic field.

2. A plane diffusion wave with regard to the Hall effect

Let the components of magnetic field depend on coordinate z only, i.e., $\mathbf{H} = \left(H_x(t,z), H_y(t,z), H_{z0}\right)$. We neglect the medium motion. Then, the magnetic field equation (for components) is written in the following form:

http://dx.doi.org/10.5772/intechopen.75713

$$\frac{dH_x}{dt} = \nu\frac{\partial^2 H_x}{\partial z^2} + \beta\frac{\partial^2 H_y}{\partial z^2}, \quad \frac{dH_y}{dt} = \nu\frac{\partial^2 H_y}{\partial z^2} - \beta\frac{\partial^2 H_x}{\partial z^2}, \quad \frac{dH_z}{dt} = 0, \quad \beta = bH_{z0}. \tag{2}$$

Consider the problem of a diffusion wave propagating in an unbounded medium with the given boundary and initial conditions:

$$\mathbf{H}(t, z=0) = \mathbf{H}_1, \quad \mathbf{H}(t, z\to\infty) = \mathbf{H}_0, \quad \mathbf{H}(t=0, z) = \mathbf{H}_0, \quad \mathbf{H}_0 = (0,0,H_{z0}), \quad \mathbf{H}_1 = \left(H_{x0}, H_{y0}, H_{z0}\right). \tag{3}$$

Let $\gamma = \sqrt{\nu^2+\beta^2}$. A general solution to Eq. (2) for the self-similar variable $\xi = z/\sqrt{4\gamma t}$ looks like

$$H_x = H_{x0} + C_1\Phi(\xi) + C_2\Psi(\xi), H_y = H_{y0} + C_1\Psi(\xi) - C_2\Phi(\xi), H_z = H_{z0}$$

where $\Phi(\xi) = \int_0^\xi \exp\left(-\nu x^2/\gamma\right)\sin\left(\beta x^2/\gamma\right)dx$, $\Psi(\xi) = \int_0^\xi \exp\left(-\nu x^2/\gamma\right)\cos\left(\beta x^2/\gamma\right)dx$.

Since $\Phi(\infty) = \Gamma\frac{1}{2}\sqrt{\frac{\gamma-\nu}{2\gamma}} = \sqrt{\frac{\pi(\gamma-\nu)}{2\gamma}}$, $\Psi(\infty) = \Gamma\frac{1}{2}\sqrt{\frac{\gamma+\nu}{2\gamma}} = \sqrt{\frac{\pi(\gamma+\nu)}{2\gamma}}$ constants C_1, C_2 with regard to boundary conditions can be found from equations

$$C_1 = \frac{-H_{x0}\Phi(\infty) - H_{y0}\Psi(\infty)}{\Phi(\infty)+\Psi(\infty)} = -\frac{2}{\sqrt{\pi}}\left(H_{x0}\sqrt{\frac{\gamma-\nu}{2\gamma}} + H_{y0}\sqrt{\frac{\gamma+\nu}{2\gamma}}\right),$$

$$C_2 = \frac{-H_{x0}\Psi(\infty) + H_{y0}\Phi(\infty)}{\Phi(\infty)+\Psi(\infty)} = -\frac{2}{\sqrt{\pi}}\left(H_{x0}\sqrt{\frac{\gamma+\nu}{2\gamma}} - H_{y0}\sqrt{\frac{\gamma-\nu}{2\gamma}}\right).$$

Simulation setup: the initial data is described by Eq. (3). A bounded computational domain $0 < z < L$, $L = 1$ is considered. For this reason, the magnetic field value taken from the analytical solution $H_x(t, z=L) = 1 + (C_1\Phi + C_2\Psi)\frac{L}{\sqrt{4\gamma t}}$, $H_y(t, z=L) = 1 + (C_1\Psi - C_2\Phi)\frac{L}{\sqrt{4\gamma t}}$, $H_z(t, z=$

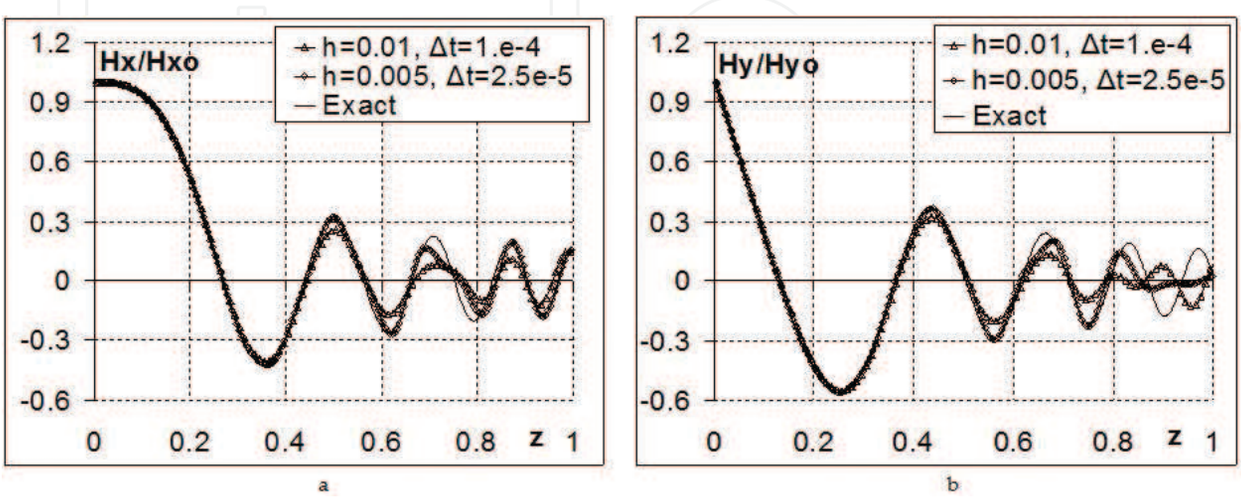

Figure 1. Profiles of field components at time $t = 0.01$: (a) H_x and (b) H_y.

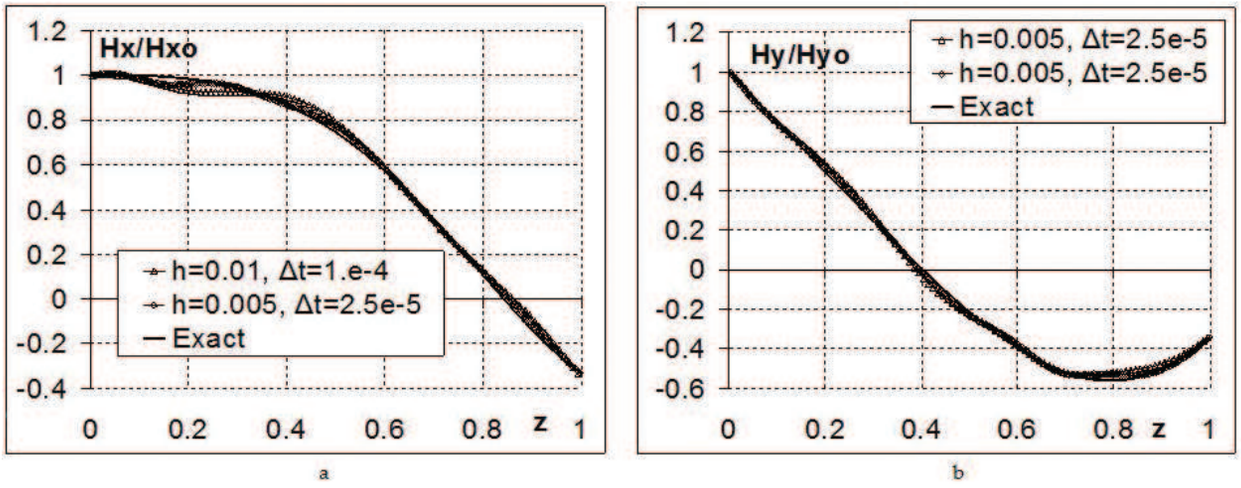

Figure 2. Profiles of field components at time $t = 0.1$: (a) H_x and (b) H_y.

$L) = 1$ is imposed on the right boundary $z = L$. On the left boundary $z = 0$, the field components take constant values according to Eq. (3). In simulations with 2D and 3D codes, boundary conditions $\partial\mathbf{H}/\partial\mathbf{n} = 0$ ($\mathbf{n}$ is a normal vector to a face) are imposed on lateral faces. By varying parameters ν and β, we can study the effect of the diffusion and Hall terms in Eq. (2) on the diffusion wave parameters. Consider an option with the Hall effect dominating over the diffusion effect: $\nu = 0$, $\beta = 1$, $H_{x0} = H_{y0} = H_{z0} = 1$. Profiles of magnetic field's components H_x, H_y at time $t = 0.01$, 0.1 are shown in **Figures 1** and **2**. With the grid refinement, convergence to the reference solution takes place.

3. Diffusion of magnetic field in an immovable plane layer of plasma with regard to joule heating and its effect on the diffusion and heat conduction coefficients

The problem of magnetic diffusion in a plane layer of material has many applications in practice [14]. In its detailed formulation, the problem was considered in paper [14] for mega gauss fields. Hydrodynamic motion, magnetic diffusion, heat conduction by electrons, and radiant heat exchange in the "back and forth" approximation were taken into account. Since finding an exact solution to such a problem causes difficulties, the original formulation needs to be simplified. Self-similar solutions to the problem obtained with simplifying assumptions were also presented in [15].

A model problem is considered with the following assumptions:

- plasma is immovable, it has a constant heat capacity,
- plasma has Coulomb conductivity,
- heat conduction is absent.

With such assumptions, the problem is reduced to solving equations

$$\frac{d\mathbf{H}}{dt} = -rot(\nu \cdot rot\mathbf{H}),\ \rho\frac{dT}{dt} = (\gamma-1)\nu(rot\mathbf{H}\cdot rot\mathbf{H}), \tag{4}$$

where $\nu = c^2/4\pi\sigma, \quad \sigma = \sigma_0(T/Ry)^\alpha, \quad \alpha = 3/2, \quad \gamma - 1 = R/C_V, \quad R = 1, \quad C_V = 1.5$

Here, ρ is the density of plasma, γ is the heat capacity ratio (adiabatic index), σ_0 is the conductivity at $T = Ry$ (it is expressed via atomic constants), and Ry is the Rydberg constant. Energy units have been chosen for temperature.

At initial time $t = 0$, all quantities depend on one space coordinate. It is assumed that the magnetic field has only one component, $\mathbf{H} = (0, 0, H_z)$. The solution is considered for the problem with initial conditions Eq. (5) and boundary conditions Eq. (6):

$$H_z(x, t=0) = \begin{cases} 0 & if \quad x < 0 \\ H_0 & if \quad x > 0 \end{cases}, T(x, t=0) = T_0, \rho(x, t=0) = \rho_0 \tag{5}$$

$$H_z(x \to -\infty, t) = 0, H_z(x \to \infty, t) = H_0, T(x \to \pm\infty, t) = T_0. \tag{6}$$

For dimensionless variables, $h_z = H_z/H_0$, $\tau = T/T_0$ Eq. (4) are reduced to the form:

$$\frac{dh_z}{dt} = \frac{\partial}{\partial x}\nu(\tau)\frac{\partial h_z}{\partial x}, \frac{d\tau}{dt} = \eta\nu(\tau)\left(\frac{\partial h_z}{\partial x}\right)^2, \nu(\tau) = \nu_0\tau^{-\alpha}, \nu_0 = \frac{c^2}{4\pi\sigma_0}\left(\frac{T_0}{Ry}\right)^\alpha, \eta = (\gamma-1)\frac{H_0^2}{\rho T_0}. \tag{7}$$

In an infinite region ($-\infty < x < \infty$), the problem has a self-similar solution depending on the variable $\xi = x/\sqrt{\nu_0 t}$. The solution can be obtained by integrating the system of ordinary differential equations:

$$\frac{\xi}{2}\frac{dh_z}{d\xi} + \frac{d}{d\xi}\left(\tau^{-\alpha}\frac{dh_z}{d\xi}\right) = 0, \frac{\xi}{2}\frac{d\tau}{d\xi} + \eta\tau^{-\alpha}\left(\frac{dh_z}{d\xi}\right)^2 = 0. \tag{8}$$

with boundary conditions

$$h_z(\xi \to -\infty) = 0, \quad h_z(\xi \to \infty) = 1, \quad \tau(\xi \to \pm\infty) = 1. \tag{9}$$

Note that for a linear case, $\alpha = 0$, the solution of Eqs. (8), (9) can be found in quadratures

$$h_z(\xi) = 0.5(1 + \text{sign}(\xi)\text{erf}(\xi/2)), \tau(\xi) = 1 - \frac{\eta}{4\pi}Ei\left(-\xi^2/4\right). \tag{10}$$

Since $Ei(-x) = C + \ln x + \sum_i \frac{(-1)^i x^i}{i\cdot i!}$, temperature in the vicinity of interface $\xi^2 \sim 0$ for the linear case $\alpha = 0$ has the logarithmic profile $\tau(\xi) \sim -\eta \ln \xi^2/4\pi$.

In general, if $\alpha > 0$, one does not manage to establish the asymptotic law for temperature in the vicinity of $\xi^2 \sim 0$, because of no integral curves of Eq. (8) satisfying the boundary conditions at infinity Eq. (9).

Now, let us build the reference solution to the problem with regard to heat conduction. In this case temperature near the interface takes a finite value. The diffusion equations and energy equation of magnetic field with regard to Joule heating and heat conduction are considered. As it was assumed earlier, all quantities depend on one space coordinate, and the magnetic field has only one component, $\mathbf{H} = (0, 0, H_z)$. For dimensionless variables, $h_z = H_z/H_0$ and $\tau = T/T_0$ equations are reduced to the forms

$$\frac{dh_z}{dt} = \frac{\partial}{\partial x}\nu_0\tau^{-\alpha}\frac{\partial h_z}{\partial x}, \frac{d\tau}{dt} = \eta\nu_0\tau^{-\alpha}\left(\frac{\partial h_z}{\partial x}\right)^2 + \frac{\partial}{\partial x}\kappa_0\tau^{\beta}\frac{\partial \tau}{\partial x}. \tag{11}$$

A self-similar solution depending on the variable $\xi = x/\sqrt{\nu_0 t}$ can be obtained by integrating the system of ordinary differential equations:

$$\frac{\xi}{2}\frac{dh_z}{d\xi} + \frac{d}{d\xi}\left(\tau^{-\alpha}\frac{dh_z}{d\xi}\right) = 0, \quad \frac{\xi}{2}\frac{d\tau}{d\xi} + \eta\tau^{-\alpha}\left(\frac{dh_z}{d\xi}\right)^2 + a\frac{d}{d\xi}\tau^{\beta}\frac{d\tau}{d\xi} = 0, \quad a = \frac{\kappa_0}{D_0}, \tag{12}$$

with boundary conditions:

$$h_z(\xi \to -\infty) = 0, \quad h_z(\xi \to \infty) = 1, \quad \tau(\xi \to \pm\infty) = 1. \tag{13}$$

To find the reference solution, it is convenient to use the first-order system with an increased number of unknowns instead of the second-order system Eq. (12). The first-order system relative to variables $h_z, \tau, \Psi = \tau^{-\alpha}dh_z/d\xi, w = -a\tau^{\beta}d\tau/d\xi$ looks like

$$\frac{dh_z}{d\xi} = \Psi\tau^{\alpha}, \quad \frac{d\tau}{d\xi} = -\frac{w\tau^{-\beta}}{a}, \quad \frac{d\Psi}{d\xi} = -\frac{\xi\Psi\tau^{\alpha}}{2}, \quad \frac{dw}{d\xi} = -\frac{\xi w\tau^{-\beta}}{2a} + \eta\Psi^2\tau^{\alpha}. \tag{14}$$

Consider the numerical solution of Eq. (14) for the right half plane ($0 < \xi < \infty$). The solution in the left half plane $(-\infty < \xi < 0)$ follows from the symmetry conditions:

$$h_z(-\xi) = 1 - h_z(\xi), \quad \tau(-\xi) = \tau(\xi), \quad \Psi(-\xi) = \Psi(\xi), \quad w(-\xi) = -w(\xi).$$

Consider the numerical solution of Eq. (14) in a bounded domain $(0 < \xi < \xi_1)$. To formulate boundary conditions for this bounded domain, it is required to find the asymptotic behavior of functions with $\xi \to \infty$. Asymptotic laws can be formulated, if we assume $a = 0.5$. In this case boundary conditions have the form:

$$\begin{aligned} &h_z(\xi \to \infty) = 0.5(1 + \mathrm{erf}(\xi/2)), \quad \tau(\xi \to \infty) = 1, \\ &\Psi(\xi \to \infty) = c_1 \exp\left(-\xi^2/4\right), \quad w(\xi \to \infty) = \left(c_2 + \eta\xi c_1^2\right)\exp\left(-\xi^2/2\right). \end{aligned} \tag{15}$$

Constants C_1, C_2 are taken so that the following conditions are satisfied on the left boundary of the computational domain:

$$h_z(\xi = 0) = 0.5, \quad w(\xi = 0) = 0.$$

Confine oneself to the consideration of case $a = 0.5$. Introduce new variables $\Psi(\xi) = \Psi(\xi) \exp\left(\xi^2/4\right)$, $W(\xi) = w(\xi) \exp\left(-\xi^2/2\right)$ with regard to boundary conditions Eq. (15). The replacement of variables gives us the equation system:

$$\frac{dh_z}{d\xi} = \Psi\tau^\alpha \exp\left(-\frac{\xi^2}{4}\right), \quad \frac{d\tau}{d\xi} = -\frac{W\tau^{-\beta}}{a} \exp\left(-\frac{\xi^2}{2}\right),$$
$$\frac{d\Psi}{d\xi} = -\frac{\xi\Psi(1-\tau^\alpha)}{2}, \quad \frac{dW}{d\xi} = \frac{\xi W\left(1-\tau^{-\beta}\right)}{2a} + \eta\Psi^2\tau^\alpha \tag{16}$$

with boundary conditions:

$$h_z(\xi = \xi_1) = 0.5(1 + \mathrm{erf}(\xi_1/2)), \quad \tau(\xi = \xi_1) = 1,$$
$$\Psi(\xi = \xi_1) = c_1, \quad W(\xi = \xi_1) = c_2 + \eta\xi_1 c_1^2, \tag{17}$$
$$h_z(\xi = 0) = 0.5, \quad w(\xi = 0) = 0.$$

The set of Eqs. (16), (17) was solved numerically with the methods of automatically selecting an integration step. The following values of parameters were used in simulations: $\xi_1 = 10$, $\eta = 20/3$, $\alpha = 3/2$, $D_0 = 1$, and $k_0 = aD_0 = 1/2$. The values of constants satisfying the boundary conditions Eq. (17) were obtained: $C_1 = 0.10231$ and $C_2 = 1.79474$. Since the behavior of functions near the right boundary corresponds to asymptotic laws Eq. (17), the reduction of parameter ξ_1 from $\xi_1 = 10$ to $\xi_1 = 1$ does not affect simulation results.

Results of simulations are illustrated in **Figures 3** and **4**. With the use of such regularity method (with regard to heat conduction), temperature at the central point of the computational domain takes its finite value. Note that with $t = 1/v_0$ the space coordinate coincides with the self-similar coordinate, $x = \xi$.

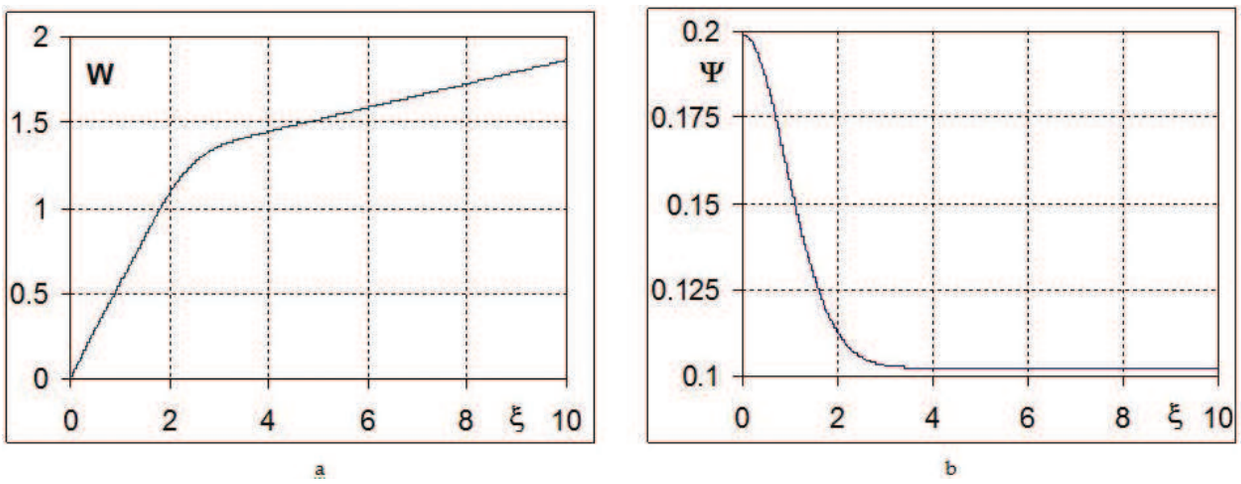

Figure 3. Profiles of self-similar functions: (a) W and (b) Ψ.

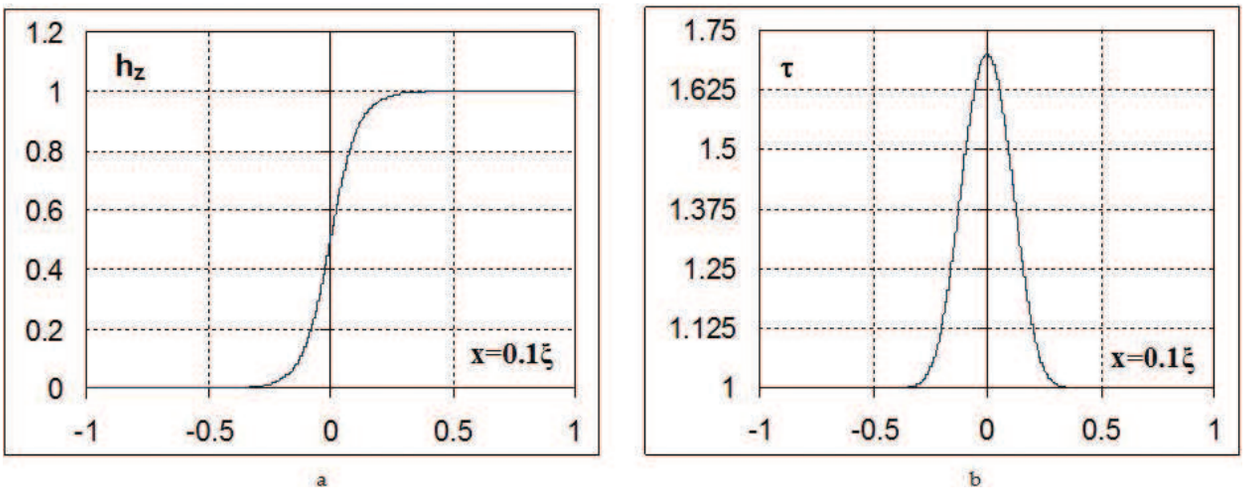

Figure 4. Profiles: (a) magnetic field and (b) temperature.

4. A point explosion in a perfectly non-conducting atmosphere

Let us consider the problem of a point blast in the presence of a uniform magnetic field (for definiteness) along the z axis ($H_z = H_{z0} = 0.01$) in a perfectly non-conducting atmosphere. Initial data are chosen in such a way that the field has no effect on the motion of matter $\varepsilon_0(r_2/r_1)^3 >> H_{z0}^2/\rho_0$. It is assumed that behind the shock front, the medium becomes perfectly conducting. If a self-similar solution to the problem of a point explosion is known, then one can calculate the magnetic field components at some time $t > 0$. In an external domain $(r > r_F(t))$, the magnetic field's vector potential is the solution to stationary equation $rot(rot\Psi) = 0$. With regard to conditions at infinity, this solution takes the form [16]:

$$\Psi_r(r,\vartheta,t) = 0, \quad \Psi_\varphi(r,\vartheta,t) = 0.5H_{z0}r\left(1 - C(t)/r^3\right)\sin\vartheta, \quad \Psi_\vartheta(r,\vartheta,t) = 0. \tag{18}$$

Here, unknown constant $C(t) = br_F^3(t)$ can be found from the condition of coupling with the solution in an internal domain $(r < r_F(t))$. Write components of magnetic field $\mathbf{H} = rot\Psi$:

$$H_r(r,\vartheta,t) = H_{z0}\left(1 - C(t)/r^3\right)\sin\vartheta, \quad H_\varphi(r,\vartheta,t) = 0, \quad H_\vartheta(r,\vartheta,t) = -H_{z0}\left(1 + 0.5C(t)/r^3\right)\cos\vartheta.$$

The solution in the internal domain ($r < r_F(t)$) is found from the freezing-in condition of the magnetic field:

$$\frac{d}{dt}\left(\frac{H_r}{\rho}\right) = \frac{H_r}{\rho}\frac{\partial u_r}{\partial r}, \quad \frac{d}{dt}\left(\frac{H_\vartheta}{\rho}\right) = \frac{H_\vartheta}{\rho}\frac{u_r}{r}, \quad \frac{d}{dt}\left(\frac{H_\varphi}{\rho}\right) = \frac{H_\varphi}{\rho}\frac{u_r}{r}.$$

The integration of these equations with regard to the solution in external domain Eq. (18) gives us

$$H_r(r,\vartheta,t) = H_{z0}h_r(r,t)\cos\vartheta, \quad H_\vartheta(r,\vartheta,t) = H_{z0}h_\vartheta(r,t)\sin\vartheta, \quad H_\varphi(r,\vartheta,t) = 0, \tag{19}$$

where

$$h_r(r,t)=\begin{cases}1-\beta\left(\frac{r_F(t)}{r}\right)^3, & r>r_F(t)\\ (1-\beta)\left(\frac{r_0(r,t)}{r}\right)^2, & r\le r_F(t)\end{cases}, h_\vartheta(r,t)=\begin{cases}-1-\frac{\beta}{2}\left(\frac{r_F(t)}{r}\right)^3, & r>r_F(t)\\ -\left(1+\frac{\beta}{2}\right)\frac{\rho(r,t)r(\gamma-1)}{\rho_0 r_0(r,t)(\gamma+1)}, & r\le r_F(t)\end{cases}.$$

Here, the functions $r_0(r,t)$, $\rho(r,t)$ are defined from the self-similar solution to the point blast problem [17].

Unknown constant β can be found from the condition of the solenoidal distribution of magnetic field in internal domain.

$$\mathrm{div}\mathbf{H}=H_{z0}\cos\vartheta\left(\frac{1}{r^2}\frac{\partial r^2 h_r}{\partial r}+2\frac{h_\vartheta}{r}\right)=2\frac{H_{z0}}{r_0}\cos\vartheta\left((1-\beta)\frac{r_0^2\partial r_0}{r^2\partial r}-\left(1+\frac{\beta}{2}\right)\frac{\rho}{\rho_0}\frac{\gamma-1}{\gamma+1}\right)=0.$$

Since $\frac{\rho}{\rho_0}=\frac{r_0^2\partial r_0}{r^2\partial r}$, then $1-\beta=\left(1+\frac{\beta}{2}\right)\frac{\gamma-1}{\gamma+1}$. That is why $\beta=\frac{4}{3\gamma+1}$.

Note that in external domain this condition is satisfied automatically. In Cartesian coordinates, the solution of Eq. (19) looks like

$$\begin{aligned}&H_x(x,y,z,t)=\frac{H_{z0}xz}{r^2}(h_r(r,t)+h_\vartheta(r,t)),\quad H_y(x,y,z,t)=\frac{H_{z0}yz}{r^2}(h_r(r,t)+h_\vartheta(r,t)),\\ &H_z(x,y,z,t)=H_{z0}\left(\frac{z^2}{r^2}(h_r(r,t)+h_\vartheta(r,t))-h_\vartheta(r,t)\right).\end{aligned}\tag{20}$$

It is convenient to compare the numerical and exact solutions using the field components depending on one space coordinate:

$$\begin{aligned}&h_r(r,t)=\frac{H_r}{H_{z0}\cos\vartheta}=\frac{1}{H_{z0}}\left(H_z(x,y,z,t)+\frac{xH_x(x,y,z,t)+yH_y(x,y,z,t)}{z}\right),\\ &h_\vartheta(r,t)=\frac{H_\vartheta}{H_{z0}\sin\vartheta}=-\frac{1}{H_{z0}}\left(H_z(x,y,z,t)-\frac{z\left(xH_x(x,y,z,t)+yH_y(x,y,z,t)\right)}{r^2-z^2}\right),\\ &h_\varphi(r,t)=\frac{H_\varphi}{H_{z0}\sin\vartheta}=\frac{1}{H_{z0}}\left(\frac{-yH_x(x,y,z,t)+xH_y(x,y,z,t)}{r}\right)=0.\end{aligned}\tag{21}$$

The magnetic field lines can be obtained by integrating equations

$$\frac{dx}{dz}=\frac{xz(h_r(r,t)+h_\vartheta(r,t))}{-r^2h_\vartheta(r,t)+z^2(h_r(r,t)+h_\vartheta(r,t))},\ \frac{dy}{dz}=\frac{yz(h_r(r,t)+h_\vartheta(r,t))}{-r^2h_\vartheta(r,t)+z^2(h_r(r,t)+h_\vartheta(r,t))}.\tag{22}$$

We consider the process stage, at which the numerical simulation becomes self-similar. In this case, the shock wave is considerably far (compared to the energy release region) from the blast center. For example, at the final time $t = 3$, the wave front is located at a distance of $R_F = 13.467$.

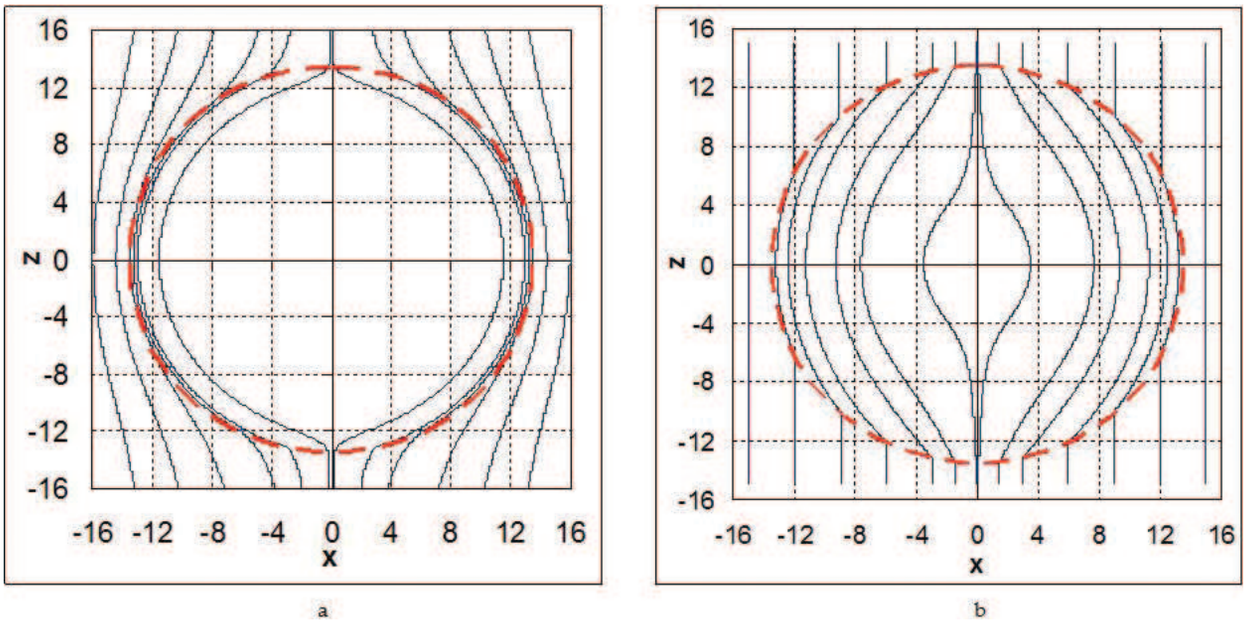

Figure 5. The magnetic field lines at time $t = 3$ in plane $y = 0$. A dashed line shows the shock front. Strong blast in a perfectly nonconducting atmosphere (a) and in a uniform conducting atmosphere (b) [11].

The flow parameters in this problem depend on a single spatial variable, r, and the field components, on two variables, r and θ. One can restrict the consideration to any plane passing through the z axis. Magnetic field lines in the plane $y = 0$ at $t = 3$ are shown in **Figure 5**. It follows from this figure that these lines of force stretch along axis z and, thereby, prevent the spread of gas in the direction orthogonal to this axis. This effect is small in the given problem because of the field smallness. With an increased strength of the field, the pressure zone gets out of its spherical shape due to occurrence of the singled out direction.

Profiles of the field components H_y and H_z along the line $x = z$ in this plane are presented in **Figure 6**. The self-similar functions of fluid parameters and radial and angular field components h_r and h_θ depend on one spatial variable r. These functions are shown in **Figure 7**. In testing numerical methods, the values of grid functions for all cells in the domain can be mapped onto the

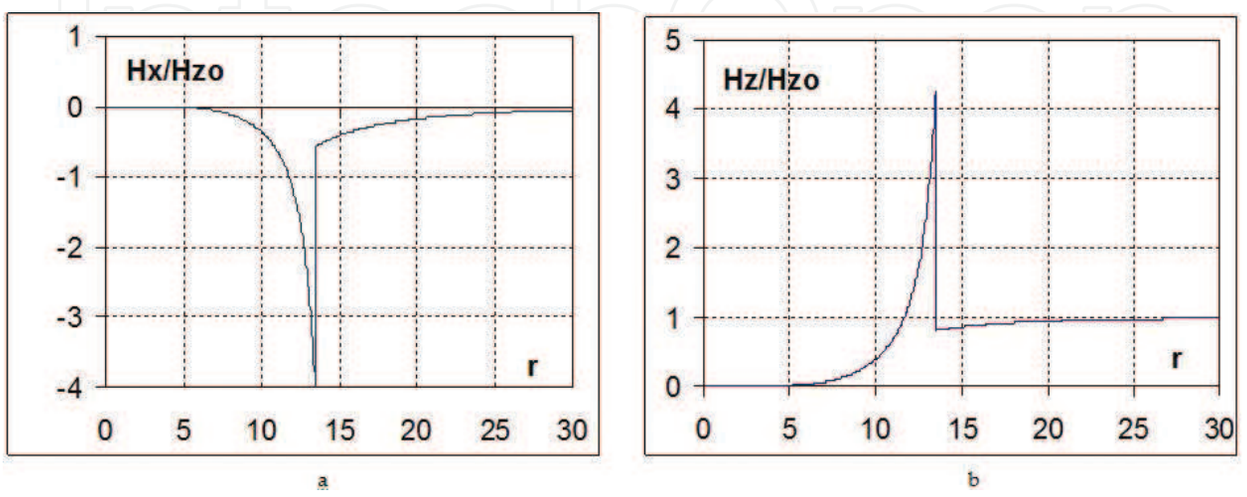

Figure 6. Profiles of field components along line $x = z$ *and* $y = 0$ at time $t = 3$: (a) H_x and (b) H_z.

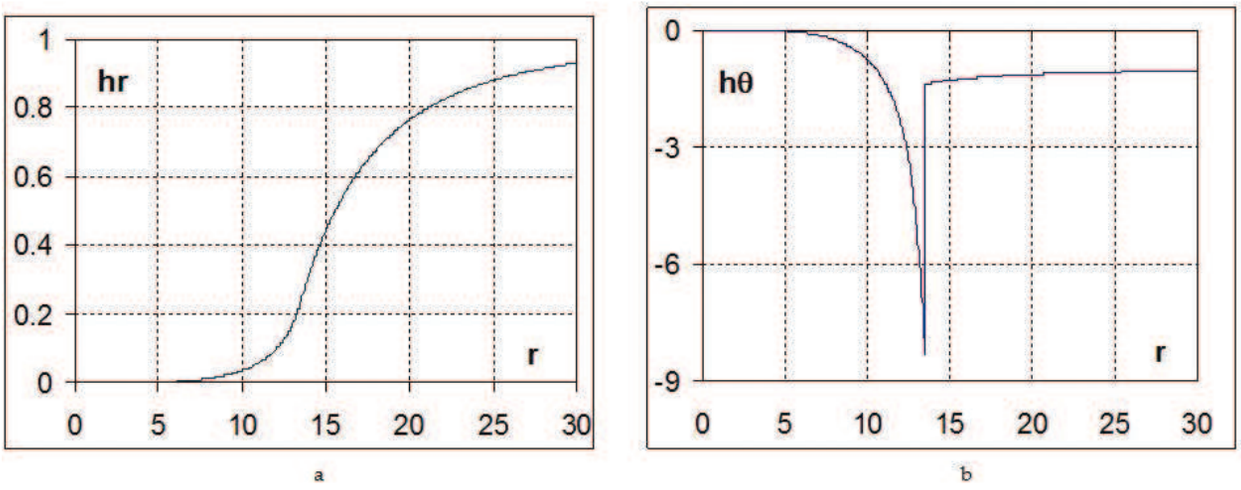

Figure 7. Profiles of the non-dimensionalized field components at time $t = 3$: (a) radial h_r and (b) angular h_θ.

figures. Such a comparison of reference versus numerical solution indicates whether the spherical symmetry is preserved during numerical simulations.

Simulation setup: The energy release region is a sphere of radius $r_1 = 0.1$, in which the initial specific energy per unit mass is set to $\varepsilon = \varepsilon_0 = 10^7$ and the initial density is set to $\rho = \rho_0 = 1$. In the spherical layer $r_1 < R < r_2 = 15$, the specific energy and the density are equal to $\varepsilon = 0$, $\rho = \rho_0 = 1$, respectively. The EOS is $P = \rho(\gamma - 1)\varepsilon$, $\gamma = 1.4$. The problem domain in the three-dimensional setup is a cube $L \times L \times L$. All boundary faces of the domain are rigid walls.

This problem requires taking into account the magnetic field diffusion in external domain (outside the shock front). It is assumed that behind the shock front, the medium becomes perfectly conducting due to ionization effects. The magnetic viscosity is approximated by the following dependence:

$$\nu(\varepsilon) = \frac{c^2}{4\pi\sigma} = \begin{cases} \nu_1 = 10^5, & \varepsilon \le 0, \\ \nu_1(1 - \varepsilon/\varepsilon_1), & 0 < \varepsilon < \varepsilon_1 = 1, \\ 0, & \varepsilon_1 \le \varepsilon. \end{cases}$$

Parameter ε_1 is chosen to provide that the magnetic viscosity behind the shock front is always zero, i.e., the condition $\varepsilon_1 < \varepsilon_F(t) \simeq \varepsilon_0 (r_1/r_F(t))^3$, $t \le t_k = 3$ is satisfied. Accounting of diffusion in external domain leads to the necessity of increasing the size of computational domain $(r_F(t_k)/L))^3 << 1$) in comparison with the ideal MHD problems to be able to set boundary conditions corresponding to the initial undisturbed state. Thus, the size of computational domain must be almost five times larger, $L \approx 75$.

5. Diffusion of magnetic field into a spherical plasma cloud

The problem formulation and its analytical solution have been taken from [16]. In contrast to this paper, consider the diffusion problem (the plasma cloud motion is neglected):

$$\frac{\partial H}{\partial t} = -rot(\nu \cdot rot\mathbf{H} + b[\mathbf{H} \times rot\mathbf{H}]). \tag{23}$$

It is assumed that the magnetic field at infinity is uniform and directed along axis z: $\mathbf{H}(0, 0, H_0 = \sqrt{2})$ (see **Figure 8**). The magnetic viscosity coefficient is constant inside and outside the cloud: $\nu(r) = \begin{cases} \nu_1, & r < r_0 = 1 \\ \nu_2, & r > r_0 \end{cases}$.

5.1. Diffusion of magnetic field in the absence of the Hall effect

Assume that the Hall effect contribution is small, $bH_0/\nu \ll 1$. Write the equation of diffusion relative to vector potential $\mathbf{H} = rot\mathbf{\Psi}$:

$$\frac{\partial \Psi}{\partial t} = -\nu \cdot rot \;\; rot\mathbf{\Psi}. \tag{24}$$

This is an axially symmetric problem, and, therefore, it is convenient to use the polar coordinate system (r, ϑ, φ). With no Hall effect and with regard to the conditions at infinity, the initial data for vector potential takes the form [16]

$$\Psi_r(r, \vartheta, t = 0) = 0, \quad \Psi_\vartheta(r, \vartheta, t = 0) = 0, \quad \Psi_\varphi(r, \vartheta, t = 0) = rf(r, t = 0)\sin\vartheta, \tag{25}$$

$$f(r, t = 0) = \frac{H_0}{2}\begin{cases} 0 & r < r_0 \\ \left(1 - (r_0/r)^3\right) & r > r_0 \end{cases}. \tag{26}$$

The solution of Eq. (24) with initial data Eq. (25) is reduced to solving Eq. (27) with initial data Eq. (26) and boundary conditions Eq. (28):

$$\frac{df}{dt} = \frac{\nu(r)}{r^4}\frac{\partial}{\partial r}r^4\frac{\partial f}{\partial r}, \tag{27}$$

$$\frac{\partial f}{\partial r}(r = 0, t) = 0, \frac{\partial f}{\partial r}(r \to \infty, t) = 0. \tag{28}$$

The solution has the form

$$\Psi_r(r, \vartheta, t = 0) = 0, \quad \Psi_\vartheta(r, \vartheta, t) = 0, \quad \Psi_\varphi(r, \vartheta, t) = rf(r, t)\sin\vartheta. \tag{29}$$

Paper [16] considers the plasma cloud interaction with the magnetic field of vacuum, and, therefore, $\nu_2 \to \infty$ is assumed. For this special case, the solution to Eq. (27) in quadratures has been obtained, and it has the forms:

$$f(r, t) = \frac{H_0}{2}\begin{cases} 1 - \frac{6}{\zeta^2}\sum_{n=1}^{\infty}\frac{(-1)^n}{(\pi n)^2}T_n(t)\cdot\left(\cos\pi n\zeta - \frac{\sin\pi n\zeta}{\pi n\zeta}\right), & 0 < \zeta = \frac{r}{r_0} < 1 \\ 1 - \frac{6}{\zeta^2}\sum_{n=1}^{\infty}\frac{1}{(\pi n)^2}T_n(t), & 1 < \zeta \end{cases}, T_n(t) = \exp\left(-(\pi n)^2\frac{\nu_1 t}{r_0^2}\right). \tag{30}$$

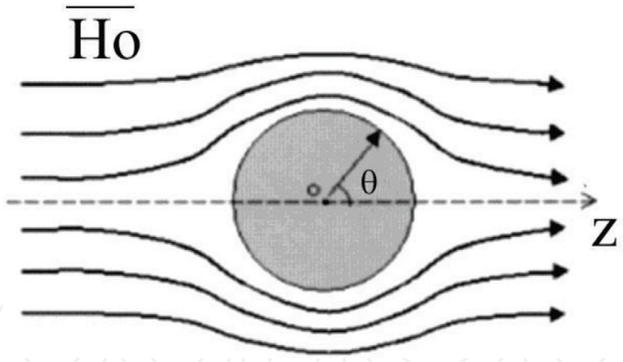

Figure 8. The problem of diffusion into a plasma cloud [16].

For finite values of conductivity in external domain $\nu_2 > 0$, the limit numerical solution of Eq. (27) has been taken for the reference solution.

Components of magnetic field $\mathbf{H} = rot\boldsymbol{\Psi}$ are found by differentiating vector potential Eq. (29). If function $f(r,t)$ is known, these components are calculated using formulas.

$$\begin{gathered} H_r(r,\vartheta,t) = h_r(r,t)\cos\vartheta, H_\vartheta(r,\vartheta,t) = -h_\vartheta(r,t)\sin\vartheta, H_\varphi(r,\vartheta,t) = h_\varphi \sin\vartheta, h_r(r,t) \\ = 2f(r,t), h_\vartheta(r,t) = \partial r^2 f/r\partial r, h_\varphi(r,t) = 0 \end{gathered} \tag{31}$$

In Cartesian coordinates the field components have the forms

$$\begin{gathered} H_z(x,y,z,t) = h_\vartheta(r,t) + \frac{z^2}{r^2}(h_r(r,t) - h_\vartheta(r,t)), H_y(x,y,z,t) \\ = \frac{zy}{r^2}(h_r(r,t) - h_\vartheta(r,t)), H_x(x,y,z,t) = \frac{xz}{r^2}(h_r(r,t) - h_\vartheta(r,t)), \end{gathered} \tag{32}$$

Since the problem is axially symmetric, any plane coming across axis z can be taken to calculate the magnetic field lines. For example, for plane $y = 0$, the differential equation describing the slope of the magnetic field lines looks like

$$\frac{dx}{dz} = \frac{xz(h_r - h_\vartheta)}{r^2 h_\vartheta + z^2(h_r - h_\vartheta)}.$$

The magnetic field lines for the reference solution at time $t = 0.01$ are shown in **Figure 9**.

Results of Eq. (32) are the formulas for the radial and angular components of the field depending on a single space coordinate:

$$\begin{gathered} h_r(r,t) = H_z(x,y,z,t) + \frac{xH_x(x,y,z,t) + yH_y(x,y,z,t)}{z}, \\ h_\vartheta(r,t) = H_z(x,y,z,t) - \frac{z\Big(xH_x(x,y,z,t) + yH_y(x,y,z,t)\Big)}{r^2 - z^2}, \\ h_\varphi(r,t) = \frac{xH_y(x,y,z,t) - yH_x(x,y,z,t)}{r} = 0. \end{gathered}$$

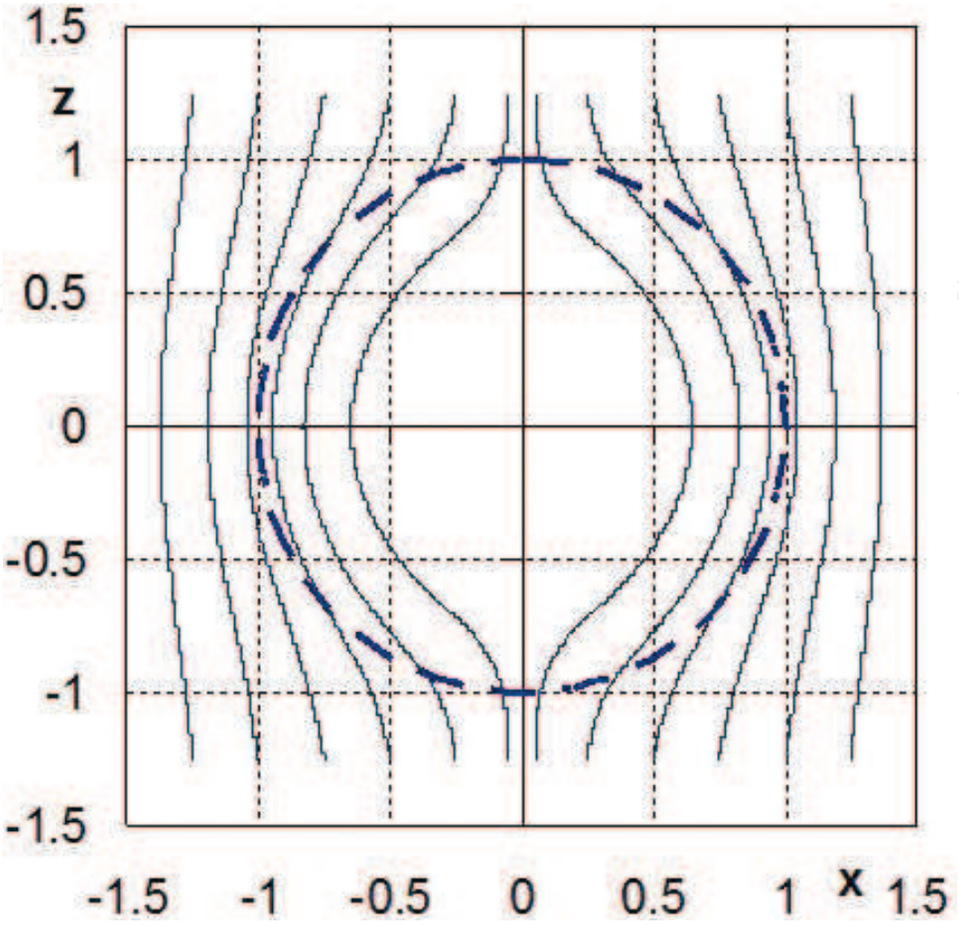

Figure 9. The magnetic field lines in the exact solution with parameters $\nu_1 = 1$ and $\nu_2 \to \infty$. A dashed line shows the plasma cloud position.

Figures 10 and **11** show profiles of field components for different magnetic viscosity values in external domain *($r > r_0$).* Note that there is a small difference between the profiles obtained with $\nu_2 = 50$ and $\nu_2 \to \infty$ corresponding to the simulation of the plasma cloud interaction with the magnetic field of vacuum $\nu_2 \to \infty$. For the problem with $\nu_2 \to \infty$, profiles of the non-dimensionalized field components for the initial phase of diffusion, $t < r_0^3/\nu_1$, are given (see **Figure 12**).

Simulation setup: A computational domain $(|x| \le 0.5L|y| \le 0.5L, |z| \le 0.5L)$ is a cube with edges $L = 10$. Boundary conditions corresponding to the initial undisturbed state are imposed on its lateral faces for the components of field $\mathbf{H}(\mathrm{r}, t)|_{\mathrm{r}\in\Gamma} = \mathbf{H}(\mathrm{r}, t = 0)$. The initial data can be set either for the magnetic field components Eq. (33) or the components of vector potential Eq. (34).

$$\begin{aligned} &H_z(x,y,z,t=0) = 2f(r,t=0) + z^2\big(1 + rf'(r,t=0)\big)/r^2, \\ &H_y(x,y,z,t=0) = xyf'(r,t=0)/r, \quad H_x(x,y,z,t=0) = xzf'(r,t=0)/r, \end{aligned} \tag{33}$$

$$\begin{aligned} &\Psi_z(x,y,z,t=0) = 0, \quad \Psi_y(x,y,z,t=0) = -zf(r,t=0), \\ &\Psi_x(x,y,z,t=0) = yf(r,t=0). \end{aligned} \tag{34}$$

http://dx.doi.org/10.5772/intechopen.75713

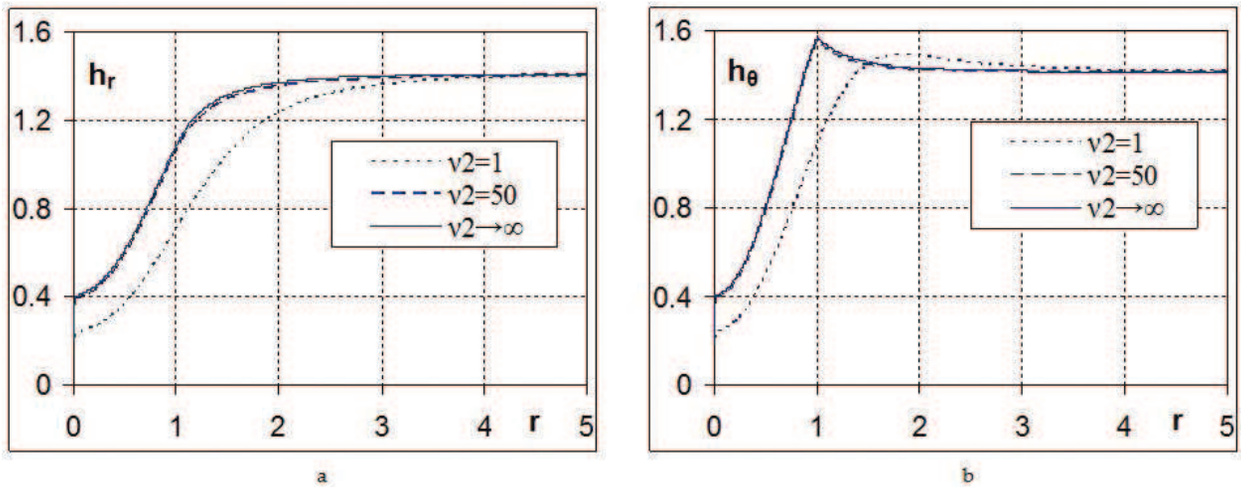

Figure 10. Profiles of the non-dimensionalized field components at time $t = 0.1$: (a) radial h_r and (b) angular h_θ.

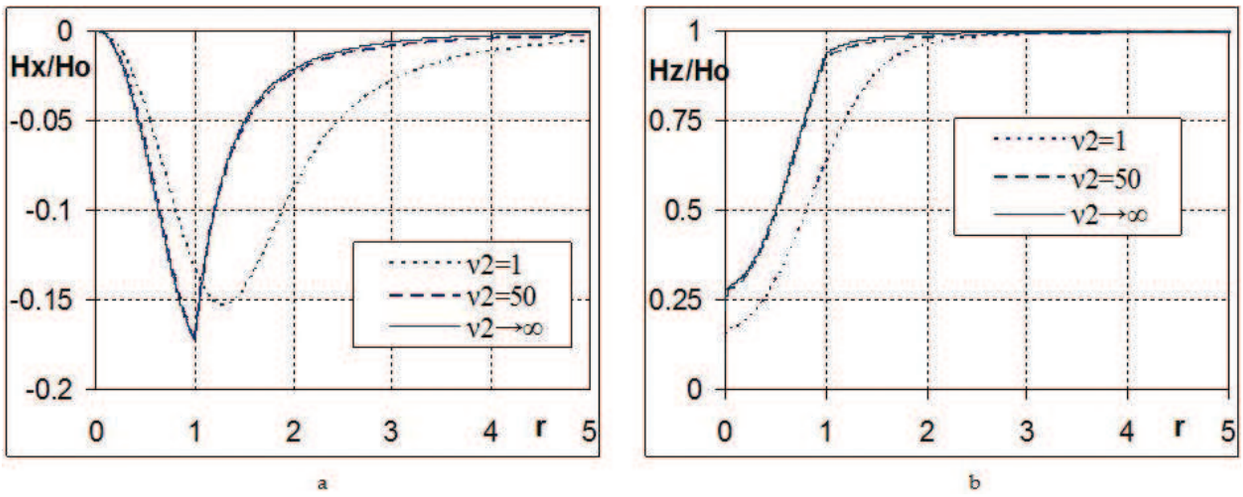

Figure 11. Profiles of the field components along line $x = z$ and $y = 0$ at time $t = 0.1$: (a) H_x and (b) H_z.

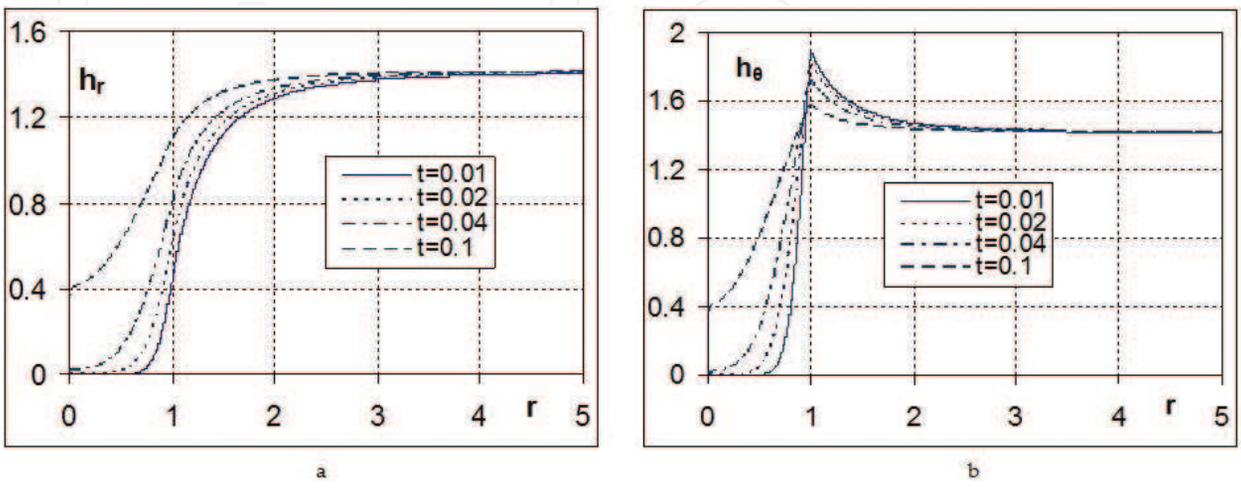

Figure 12. Evolution of non-dimensionalized field components in the problem with parameters $\nu_1 = 1$ and $\nu_2 \to \infty$: (a) radial h_r and (b) angular h_θ.

The EGIDA code uses a scheme preserving the field divergence at one step because difference operators *DIV* and *ROT* (*div* and *rot*) [18] determined at nodes and in cells of a grid, respectively, satisfy the vector analysis identities: *DIVrot = 0* and *ROTdiv = 0*.

It has been found that for the first set of initial data the divergence norm depends on errors induced by the initial distribution of the **H** field components in the vicinity of sphere $r = r_0$. Though the difference scheme does not change the magnetic field divergence, initial errors lead to a significantly distorted numerical solution (see **Figure 13**).

In the second case, the magnetic field components are determined using the operator numerically differentiating the vector potential, and, hence, the magnetic field divergence norm equals zero at initial time and at all later times. For this case, a good agreement between the calculated results and the exact solution has been achieved even on the coarsest grid (see **Figure 14**).

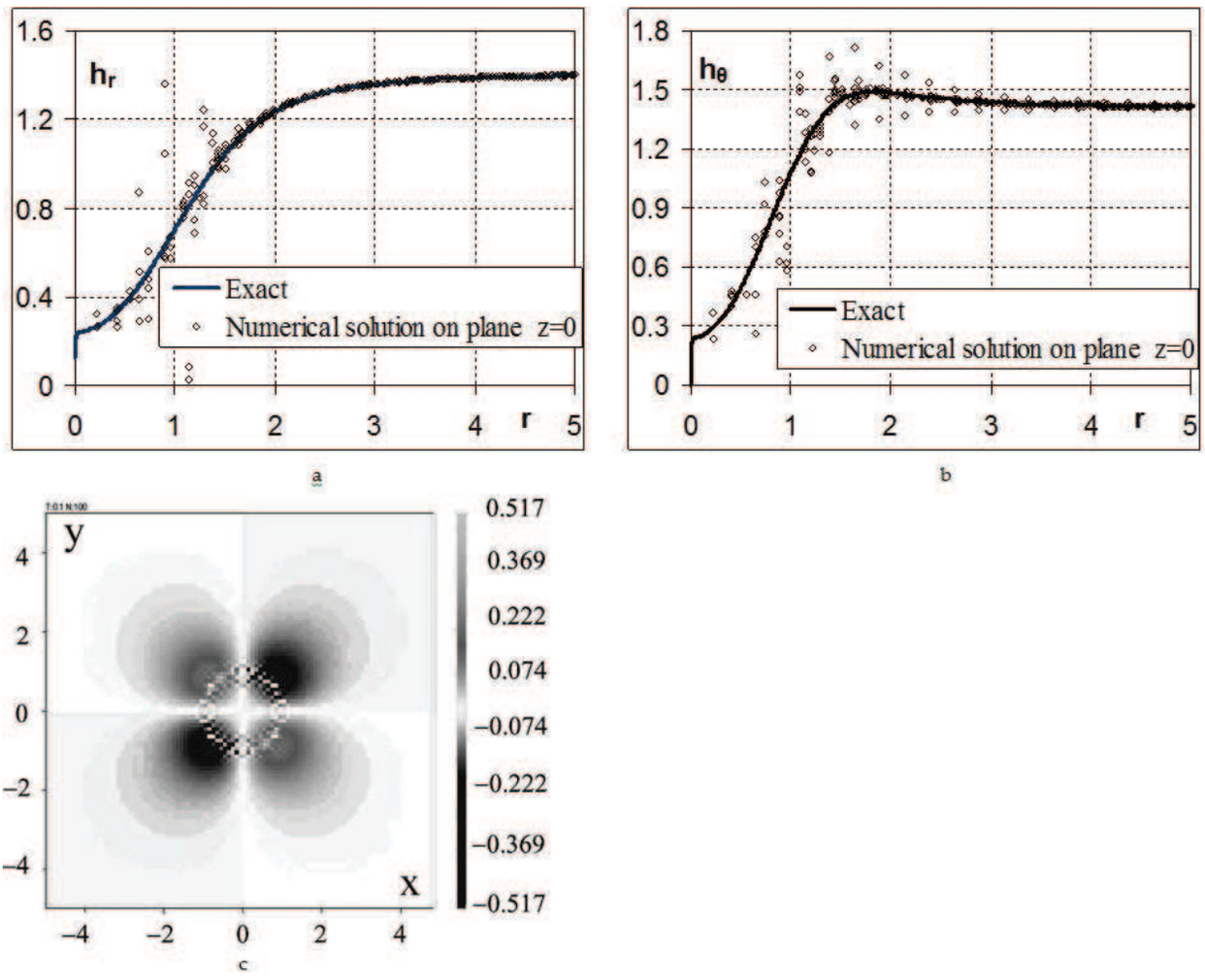

Figure 13. Calculation of the magnetic field diffusion into a spherical plasma cloud for the first set of initial data (33). Profiles of the field components at time $t = 0.1$: (a) radial h_r and (b) angular h_θ. Distribution of transverse field component H_y in section z = 0 (c).

http://dx.doi.org/10.5772/intechopen.75713

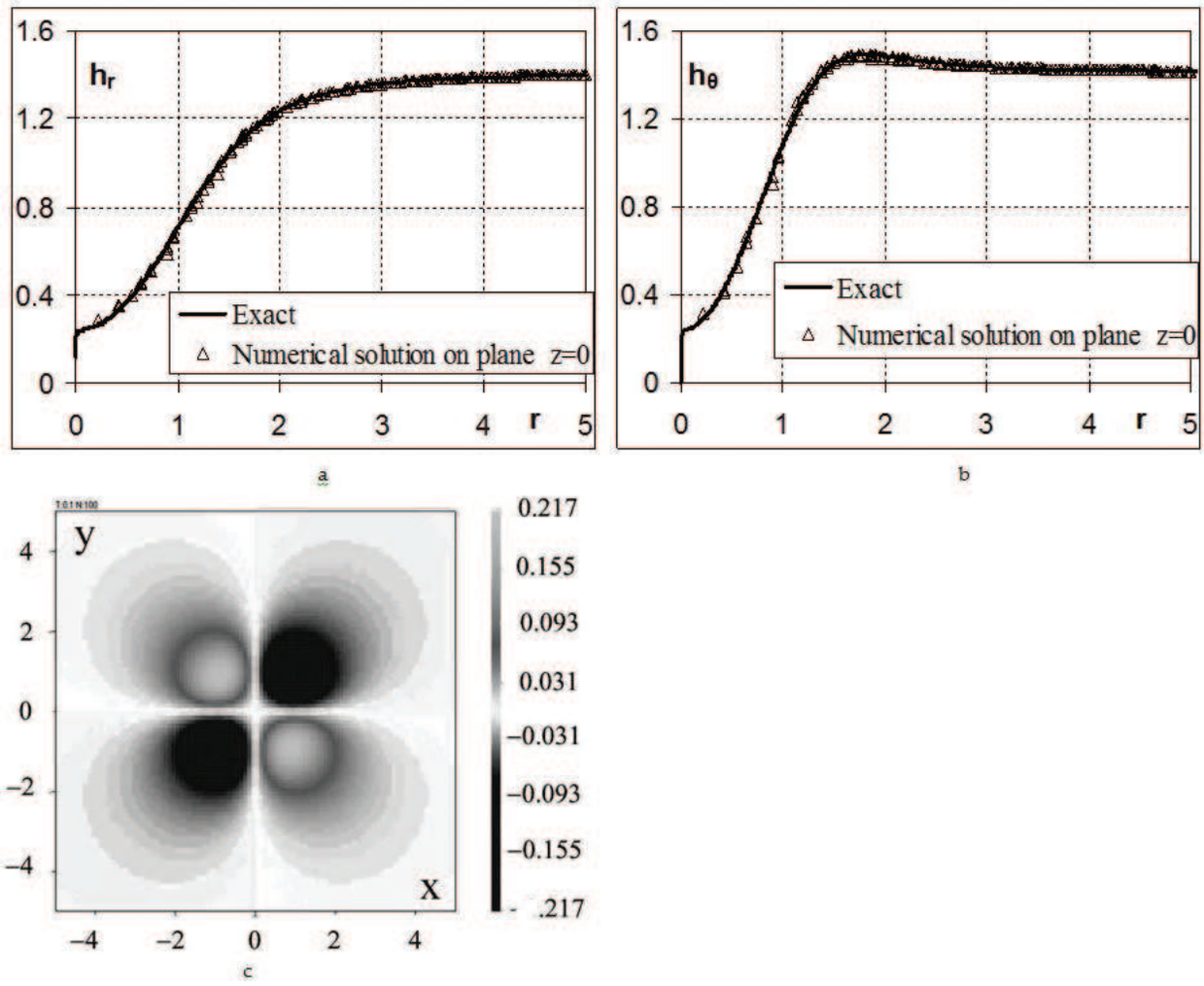

Figure 14. Calculation of the magnetic field diffusion into a spherical plasma cloud for the second set of initial data (34). Profiles of the field components at time $t = 0.1$: (a) radial h_r and (b) angular h_θ. Distribution of transverse field component H_y in section $z = 0$ (c).

5.2. Diffusion of magnetic field with a low Hall effect

Assume that the Hall effect contribution is small, $bH_0/\nu \ll 1$, but finite. For this reason, it is required to take into account the Hall term in the diffusion equation:

$$\frac{\partial \Psi}{\partial t} = -\nu \cdot rot \ \ rot\Psi - b[rot\Psi \times rot \ \ rot\Psi].$$

The Hall effect leads to the occurrence of the azimuthal component, H_φ, of magnetic field in plasma [16]:

$$H_r(r,\vartheta,t) = h_r(r,t)\cos\vartheta, H_\vartheta(r,\vartheta,t) = -h_\vartheta(r,t)\sin\vartheta, H_\varphi(r,\vartheta,t)$$
$$= h_\varphi \sin\vartheta, h_r(r,t) = 2f(r,t), h_\vartheta(r,t) = \partial r^2 f/r\partial r, h_\varphi(r,t) = \Psi(r,t)/r.$$

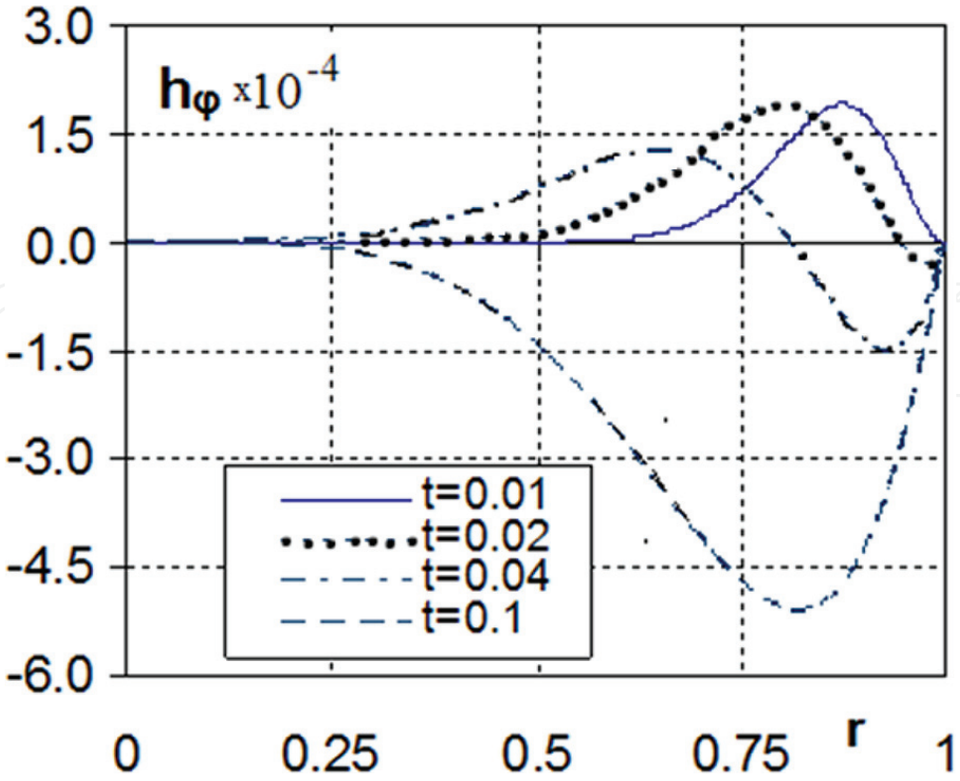

Figure 15. Profiles of the azimuthal component of non-dimensionalized field in the problem with parameters $\nu_1 = 1,\ \nu_2 \to \infty,\ b = 0.01$.

In view of the smallness of parameter bH_0/ν_1, we have Eqs. (27), (28) to calculate function $f(r,t)$, while the calculation of small additive Ψ is reduced to solving the following boundary value problem:

$$\frac{d\Psi}{dt} = \frac{\partial}{\partial r}\nu\frac{\partial\Psi}{\partial r} - \frac{6\nu\Psi}{r^2} - 2fr^2\frac{\partial}{\partial r}\left(\frac{b}{r^4}\frac{\partial}{\partial r}r^4\frac{\partial f}{\partial r}\right), \Psi(r,t=0) = 0, \Psi(r=0,t) = 0, \Psi(r\to\infty,t) = 0.$$

Figure 15 shows profiles of the non-dimensionalized azimuthal field component h_φ at early times, $t < r_0^2/\nu_1$. With small values of parameter bH_0/ν_1, the rest two components—h_r, h_ϑ—remain unchanged, and they are shown in **Figure 12**. Note that, as it has been shown in [16], if the motion of plasma is accounted, the Hall effect may lead to the occurrence of azimuthal velocity, i.e., to the plasma cloud rotation.

The changeover to Cartesian coordinates is performed using formulas

$$H_z(x,y,z,t) = h_\vartheta(r,t) + z^2(h_r(r,t) - h_\vartheta(r,t))/r^2,$$
$$H_y(x,y,z,t) = zy(h_r(r,t) - h_\vartheta(r,t))/r^2 + xh_\varphi(r,t)/r,$$
$$H_x(x,y,z,t) = xz(h_r(r,t) - h_\vartheta(r,t))/r^2 - yh_\varphi(r,t)/r.$$

Simulation setup: The initial data is given in the previous section. This problem requires accounting the Hall effect. A local exchange parameter is $b = 0.01$. **Figure 15** shows profiles of the azimuthal component of non-dimensionalized field.

6. Conclusion

An important property of difference schemes in multidimensional flow simulations is that they keep the magnetic field divergence-free in difference solutions. An adverse aspect of this defect is the unphysical transport of matter orthogonal to the field **H** [2].

Note that the zero-divergence requirements to difference schemes get more stringent as applied to the solution of diffusion problems. A violation of this requirement results in the accumulation of errors and loss of solution structure, especially in problems with high conductivity gradients.

Acknowledgements

Some EGIDA calculations have been performed under contract no. 1239349 between Sandia National Laboratories and RFNC-VNIIEF. The authors thank sincerely M. Pokoleva for her assistance in simulations and J. Kamm and A. Robinson for their assistance in formulating some benchmarks and references.

Author details

Sofronov Vasily, Zhmailo Vadim and Yanilkin Yury*

*Address all correspondence to: n.yanilkina@mail.ru

VNIIEF, Sarov, Russia

References

[1] Kulikovsky AG, Pogorelov NV, Semenov AY. Mathematical Issues of Numerical Solution of Hyperbolic Equations. Moscow: Fizmatlit; 2001 (In Russian)

[2] Brushlinsky KV. Mathematical and Computational Problems of Magnetic Gas Dynamics. Moscow: Binom; 2009 (in Russian)

[3] Balsara DS, Spicer DS. A staggered mesh algorithm using high Godunov fluxes to ensure solenoidal magnetic fields in magneto hydrodynamics simulations. Journal of Computational Physics. 1999;**149**:270-292

[4] Toth G. The ∇B=0 constraint in shock–capturing magneto hydrodynamics codes. Journal of Computational Physics. 2000;**161**:605-652

[5] Gardiner TA, Stone JM. An unsplit Godunov method for ideal MHD via constrained transport. Journal of Computational Physics. 2005;**205**:509-539

[6] Dai W, Woodward PR. An approximate Riemann solver for ideal magneto hydrodynamics. Journal of Computational Physics. 1994;**111**:354-372

[7] Brio M, Wu CC. An upwind differencing scheme for the equations of ideal magnetohydrodynamics. Journal of Computational Physics. 1988;**75**:400-422

[8] Takahashi K, Yamada S. Regular and non-regular solutions of the Riemann problem in ideal magnetohydrodynamics. Journal of Plasma Physics. 2013;**75**(3):335-356

[9] Niederhaus JHI. Code verification for ALEGRA using ideal MHD Riemann problems. Sandia National Laboratories preprint SAND2012-1362P. 2008:1-44

[10] Orszag A, Tang C. Small-scale structure of two–dimensional magneto hydrodynamics turbulence. Journal of Fluid Mechanics. 1979;**90**:129-143

[11] Zhmailo VA, Sofronov VN, Yanilkin YV. Magneto hydrodynamic test problem. Voprosy Atomnoi Nauki i Tekhniki. Ser. Teoreticheskaya I Pricladnaya Fisika. 2017;**2**:55-81 (in Russian)

[12] Yanilkin YV, Belyaev SP, Bondarenko Yu A et al. EGAK and TREK Eulerian codes for multidimensional multimaterial flow simulations. Transactions of RFNC-VNIIEF. Research publication. Sarov: RFNC-VNIIEF; 2008. **12**:54-65 (in Russian)

[13] Eguzhova MY, Zhmailo VA, Sofronov VN, Chernysheva ON, Yanilkin YV, Glazyrin SI. Implementation, analysis and testing of three–dimensional computational methods for MHD simulations of compressible multimaterial flow in Eulerian variables. In: Proceedings of the 10th Seminar on New Models and Hydro codes for Shock Wave Processes on Condensed Matter; July 27-August 1, 2014; Pardubice. Czech Republic. pp. 165-176

[14] Garanin SF, Ivanova GG, Karmishin DV, Sofronov VN. Diffusion of a mega gauss field into a metal. Journal of Applied Mechanics and Technical Physics. 2005;**46**(N2):153-159

[15] Garanin SF. Diffusion of a strong magnetic field into a dense plasma. Journal of Applied Mechanics and Technical Physics. 1985;**26**(N3):308-312

[16] Zhmailo VA, Kokoulin ME. The hall effect in the problem of plasma cloud spread in the magnetic field. Voprosy Atomnoi Nauki i Tekhniki. Ser. Teoreticheskaya I Pricladnaya Fisika. 2004;**1-2**:3-12 (in Russian)

[17] Sedov LI. Conformity and Dimensionality Methods in Mechanics. Nauka; 1977 (In Russian)

[18] Samarsky AA, Tishkin VF, Favorsky AP, Shashkov MY. Operator difference schemes. Differential Equations. 1981;**XVII**:N7 (in Russian)